Advanced Robotics, Vol. 9, No. 5, pp. 561–577 (1995)

Dexterity measures with unilateral actuation constraints: the $n+1$ case

RONALD KURTZ and VINCENT HAYWARD

Research Center for Intelligent Machines, McGill University, 3480 University Street, Montréal, Quebec H3A 2A7, Canada

Received for *AR* 12 April 1994; accepted 20 September 1994

Abstract—The study of the instantaneous kinematics and statics aims at capturing the properties of mechanisms in terms of the mapping of forces, velocities and error propagation. Dexterity measures have been developed to quantify these properties with a view to analysis and design. Tendons and cables may be viewed as unilateral actuators because they require tensioning for normal operation. When power grasping is abstracted to a set of forces acting at discrete points on the surface of an object, it can be analyzed in terms of unilateral statics. It is also used to analyze magnetic levitation resulting from forces caused by variable reluctance magnetic circuits, as is the case of a vehicle propelled by reaction jets. For all these cases, a new set of measures based on the unilateral statics is developed when $n+1$ forces act on a n d.o.f. mechanism and force mapping properties are studied. It is proposed to replace the ordinary concepts of dexterity, singularity, isotropy, maximum force amplification and maximum dexterity gradient by *unilateral dexterity*, *unilateral singularity*, *unilateral isotropy*, *unilateral maximum force amplification* and *unilateral maximum dexterity gradient*, respectively. As an example of their application, the geometric optimization of a 3 d.o.f. tendon mechanism is performed.

1. INTRODUCTION

We consider the case of a class of mechanisms which share the property that they will work only under the condition that the driving forces are all positive. For example, tendons can be viewed as unilateral actuators [1]; grasping forces applied to a solid object by a set of fingers with point contacts fall under the same description [2]; in micro-manipulation, the use of variable reluctance magnetic servo levitation has the same constraints [3]; so do jet propelled vehicles [4]. In all these cases, the unilateral force constraints cause dexterity measures to be more complicated than those of bi-directionally actuated mechanisms.

There are many advantages to unilaterally actuated mechanisms and, in some cases, there is no other alternative. In the case of tendon transmissions, actuators can be 'remotized'. The dynamics of actuated mechanisms can thus be improved, although it sometimes leads to rather complicated designs. Many examples of the successful application of this technique are found and many working tendon systems exist, most notably the human hand. As biological counterparts to man-made mechanisms, such

joints found in vertebrates and many invertebrates animals are tendon driven, giving proof by existence that such arrangements can be quite effective. Historical examples of cables of tendon driven mechanisms abound and their origins can be traced back to some of the earliest known human implements: bows for example, which exploit beautifully the phenomenon of unilateral singularity about to be discussed.

In the robotics area, mechanical hands such as the Stanford/JPL hand [1] and the Utah/MIT dextrous hand [5] use tendons exclusively. There are also applications of tendon transmissions in the field of force reflecting hand controllers for telemanipulation because tendons provide a zero backlash high efficiency environment essential for quality force transmission, as was explored by Vertut and colleagues [6]. Morecki and co-workers also implemented efficient cable driven manipulators [7], so did Takase and associates [8], and Hirose and Ma [9], citing just a few examples among many. For micro-manipulation, the use of magnetic servo levitation has been used to provide a friction-free and backlash-free motion control [3]. In the case of grasping, coordination algorithms have been proposed that enforce the unidirectionality of constraint forces [10]. More recent work on the control of tendon driven mechanisms is reported in [11, 12].

For these mechanisms to work properly, the applied forces must all remain positive. One method to achieve this is to supply a biasing force using $n + 1$ acting points when the number of degrees of freedom of the mechanism is n. The measures that we develop apply to this case. In this category, we find, for example, the cited Stanford/JPL design, as well as the six string suspended manipulator proposed in [13], in which the gravity force vector plays the role of a biasing tendon of infinite length, so to speak.

In order to exemplify the use of the developed measures, we study in some detail the case of a spherical manipulator driven by four tendons and suggest the best designs for this case.

2. STATICS OF TYPE $n+1$ UNILATERALLY CONSTRAINED MECHANISMS

It is known that 'a rigid body with n degrees of freedom can be completely constrained by $n+1$ point contacts' [14]. It is easy to show why n forces acting at discrete points are insufficient for this task. Consider the relation relating applied forces $\boldsymbol{f}$ to an external wrench $\boldsymbol{w}$ under conditions of static equilibrium:

$$\boldsymbol{w} = \boldsymbol{J}^{\mathrm{T}} \boldsymbol{f}. \tag{1}$$

As it is conventionally done in robotics, we call $\boldsymbol{J}$ the Jacobian matrix which maps the velocities of the constrained body into velocities of the actuators. The relationship holds for any structure since velocities always instantaneously map into velocities, regardless of the coordinates which are selected. Because we are concerned by statics, it is well known that following the principle of virtual works, the above transposed relationship maps forces and torques under the conditions of static equilibrium, regardless as well of the coordinates which are selected.

If the mechanism is not at a singular configuration the $n \times n$ Jacobian will be invertible and thus

$$\boldsymbol{f} = \boldsymbol{J}^{-\mathrm{T}}\boldsymbol{w}, \tag{2}$$

where $\boldsymbol{J}^{-\mathrm{T}}$ is the inverse of the transpose of the Jacobian. Say for some particular $\boldsymbol{w}$ all the applied forces are positive. If the wrench $-\boldsymbol{w}$ is applied to the constrained body, then all the applied forces must be negative, violating the unilateral constraints:

$$\boldsymbol{f}_i \geqslant 0, \quad i = 1, \ldots, n, \tag{3}$$

where $\boldsymbol{f} = [\boldsymbol{f}_1, \boldsymbol{f}_2, \ldots, \boldsymbol{f}_n]^{\mathrm{T}}$. Thus n forces are not enough to control the mechanism independently of the applied wrench. Now consider the case of $n + 1$ forces for the same mechanism. Here the Jacobian is not invertible, but using the pseudo-inverse we always have:

$$\boldsymbol{f} = \boldsymbol{J}^{+}\boldsymbol{w} + \lambda \boldsymbol{h}, \tag{4}$$

where $\boldsymbol{h}$ is a vector in the nullspace of the Jacobian and λ is a free parameter. As long as all the components of $\boldsymbol{h}$ are positive, λ can be set sufficiently large to ensure that all the applied forces are positive, regardless of $\boldsymbol{w}$. Keeping the elements of $\boldsymbol{h}$ greater than zero is a necessary and sufficient condition for the quasi-static stability of the mechanism. Qualitatively the extra force is needed to supply a bias to bring all the forces in the positive range.

In general, these additional constraints contribute to reduce the workspace of unilaterally actuated mechanisms when compared to their bi-directionally actuated counterparts. Consider, for example, the two-tendon crank system in Fig. 1(b) derived from the piston example of Fig. 1(a). Here, the crank can be controlled through a limited angle, whereas in the piston case, there is no limit on the control of the rotation.

It has been shown on a simple example that unilaterally actuated mechanisms have constraints that affect statics and workspace. It is not surprising that conventional dexterity measures are not applicable to this situation. A new dexterity measure for this case will be proposed in the next section.

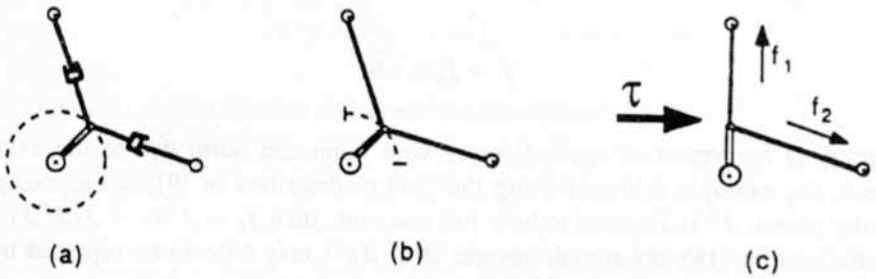

Figure 1. Crank mechanism driven by two pistons (a) and the corresponding tendon implementation (b). The range of rotation of the tendon design is inherently limited (dashed line). At the edge of the workspace the tendons cannot resist even the smallest torque in the indicated direction (c).

3. UNILATERAL DEXTERITY AND OTHER CONCEPTS

The importance of dexterity measures for finding optimal working points, postures, path planning and robot design has been often pointed out [15–17]. Therefore there is considerable motivation for investigating dexterity measures of unilateral actuation as well. The applied forces will be investigated as a means of quantifying dexterity of a tendon driven mechanism.

The condition number is a common measure of dexterity, but it does not apply to unilateral actuation. This can be seen by looking at a tendon-actuated crank when it is at the limit of its workspace (Fig. 1(c)). No amount of pulling at the tendons can resist even the smallest of torques in the indicated direction. A similar situation would occur should the crank be maneuvered by two fingers that could only push in one direction, as it is the case with cranks having a rolling handle (e.g. pencil sharpeners). Obviously, this is a very poorly conditioned configuration. This dexterity measure does not reflect this fact, as the singular value at this location is non-zero. In fact, if pistons replaced the tendons, then this configuration would be well conditioned.

A new dexterity measure is now derived to deal with this problem. It is desirable to have a measure with the same physical significance as the condition number, giving an upper bound on the propagation of errors in the linear system (2) as in [15]:

$$\frac{\|\delta \boldsymbol{f}\|}{\|\boldsymbol{f}\|} \leqslant k(\boldsymbol{J}) \frac{\|\delta \boldsymbol{w}\|}{\|\boldsymbol{w}\|}, \tag{5}$$

where $\boldsymbol{w}$ is an external wrench applied to the mechanism, $\boldsymbol{f}$ is the vector of tendon forces, and $k(\boldsymbol{J})$ is the condition number of the Jacobian matrix calculated as

$$k(\boldsymbol{J}) = \frac{\sigma_1}{\sigma_n}, \tag{6}$$

where $\sigma_1 \geqslant \cdots \geqslant \sigma_n \geqslant 0$ are the singular values of the matrix $\boldsymbol{J}$. Consider the case of $n+1$ applied forces controlling an n d.o.f. device. Starting with (4) we write:

$$\boldsymbol{f} = \boldsymbol{f}_{\mathrm{e}} + \lambda \widehat{\boldsymbol{h}}, \tag{7}$$

where $\boldsymbol{f}_{\mathrm{e}}$ is the vector of applied forces with minimum norm due to the external wrench, for example achieved using the control described in [9], since, except at singular points, $\boldsymbol{J}^{\mathrm{T}}$ is assumed to have full row rank, then $\boldsymbol{f}_{\mathrm{e}} = \boldsymbol{J}^{+}\boldsymbol{w} = \boldsymbol{J}(\boldsymbol{J}^{\mathrm{T}}\boldsymbol{J})^{-1}\boldsymbol{w}$. As discussed in [18], the pseudo inverse $\boldsymbol{J}(\boldsymbol{J}^{\mathrm{T}}\boldsymbol{J})^{-1}$ may have to be replaced by its weighted version $\boldsymbol{W}\boldsymbol{J}(\boldsymbol{J}^{\mathrm{T}}\boldsymbol{W}\boldsymbol{J})^{-1}$ and 2-norms by weighted norms to insure invariance with respects to units. However, for clarity, we will use the ordinary pseudo inverse in the rest of this discussion since it has no bearing on the form of the results.

Also, $\hat{h}$ is a *unit* vector in the nullspace of the Jacobian with all its elements positive, and by definition orthogonal to f_e. That is,

$$\hat{h} = [h_1, h_2, \ldots, h_{n+1}]^T \quad \text{such that} \quad h_i > 0, \quad i = 1, \ldots, n+1, \tag{8}$$

$$J^T \hat{h} = 0, \tag{9}$$

$$\|\hat{h}\| = 1, \tag{10}$$

$$\hat{h} \cdot f_e = 0. \tag{11}$$

The vector $\hat{h}$ can be calculated from the Jacobian as:

$$\hat{h} = \frac{(1 - J(J^T J)^{-1} J^T) z}{\|(1 - J(J^T J)^{-1} J^T) z\|}, \quad z \neq 0, \tag{12}$$

where z is an arbitrary vector with a non-zero nullspace component.

From (7), (10) and (11):

$$\|f\| = \sqrt{\|f_e\|^2 + \lambda^2}. \tag{13}$$

From the singular value decomposition theorem we can place bounds on $\|f_e\|$:

$$\frac{\|w\|}{\sigma_1} \leqslant \|f_e\| \leqslant \frac{\|w\|}{\sigma_n}. \tag{14}$$

Using (13) and (14) we place a lower bound on the tendon forces in terms of the applied wrench and the maximum singular value of the Jacobian:

$$\|f\| \geqslant \|f_e\| \geqslant \frac{\|w\|}{\sigma_1}. \tag{15}$$

An upper bound on the applied forces will now be derived. Clearly λ can be made arbitrarily large, but it would be preferable to find the minimum value of λ that satisfies all the constraints. This procedure will minimize the applied forces regardless of the external wrench. The constraints $f_i > 0$ lead to:

$$\lambda \geqslant \frac{-f_{ei}}{\hat{h}_i}, \quad i = 1, \ldots, n+1. \tag{16}$$

The minimum value of λ that satisfies these constraints is:

$$\lambda_m = \max_i \left(\frac{-f_{ei}}{\hat{h}_i} \right). \tag{17}$$

The minimum value of λ that satisfies all the constraints independent of f_e is given by

$$\lambda^* = \max_{f_e}(\lambda_m) = \max_{f_{ei}} \frac{-f_{ei}}{\hat{h}_i}. \tag{18}$$

The magnitude of f_e can be bounded as in (14), but the direction of f_e can be specified arbitrarily. In the worst case f_e is largest in the direction where the nullspace vector is smallest. Thus,

$$\lambda^* = \frac{\max_{f_e}(-f_{ei})}{\min_i\left(\hat{h}_i\right)} \tag{19}$$

$$\leqslant \frac{\|w\|}{\sigma_n h_{\min}}, \tag{20}$$

where $h_{\min} = \min_i\left(\hat{h}_i\right)$ and σ_n is the smallest singular value. From (13) and (20) an upper bound can be placed on the applied forces as follows:

$$\|f\| \leqslant \sqrt{\|f_e\|^2 + \lambda^{*2}}. \tag{21}$$

Thus

$$\|f\| \leqslant \frac{1}{\sigma_n}\frac{\sqrt{h_{\min}^2 + 1}}{h_{\min}}\|w\|. \tag{22}$$

Similarly, if we apply a small perturbation δw to the system the resulting applied forces are bounded by:

$$\|\delta f\| \leqslant \frac{1}{\sigma_n}\frac{\sqrt{h_{\min}^2 + 1}}{h_{\min}}\|\delta w\|. \tag{23}$$

From the lower bound of (15) we have

$$\frac{1}{\|f\|} \leqslant \frac{\sigma_1}{\|w\|}. \tag{24}$$

Combining (24) and (23) we arrive at the final result,

$$\frac{\|\delta f\|}{\|f\|} \leqslant k(J)\frac{\sqrt{h_{\min}^2 + 1}}{h_{\min}}\frac{\|\delta w\|}{\|w\|}, \tag{25}$$

where $k(J) = \sigma_1/\sigma_n$ is the condition number of the Jacobian.

The quantity $k(J)\sqrt{h_{\min}^2 + 1}\,/h_{\min}$ plays the same role as the condition number for bidirectional systems. In fact this measure incorporates the condition number itself. The maximum value of $h_{\min}$ subject to constraint (8) and (10) occurs when all the elements of $\hat{h}$ are equal to $1/\sqrt{n+1}$. Thus the *local unilateral dexterity* measure $\mathrm{UD_l}$ is defined as:

$$\mathrm{UD_l} \equiv \begin{cases} \sqrt{n+2}\,\dfrac{1}{k(J)}\,\dfrac{h_{\min}}{\sqrt{h_{\min}^2 + 1}} & \text{for} \quad h_{\min} \geqslant 0, \\ 0, & \text{when} \quad h_{\min} < 0. \end{cases} \tag{26}$$

This measure is normalized such that $0 \leqslant \mathrm{UD_l} \leqslant 1$. It is zero when the Jacobian is singular or when condition (8) is violated. This will be referred to as an *unilateral singularity* as it has all the properties of regular singularities including large actuator forces for small external wrenches. The 'unilateral dexterity' is one when the linear system is isotropic, $k(\boldsymbol{J}) = 1$, and when the nullspace vector is uniform in all directions, that is when $\widehat{\boldsymbol{h}} = (1/\sqrt{n+1})[1, 1, \ldots, 1]^{\mathrm{T}}$. Stated in terms of condition (9) the columns of the Jacobian must sum to zero. This will be referred to as *unilateral isotropy*.

Recall that in [13] the measure

$$F_{\mathrm{l}} = \frac{1}{\sigma_n} \tag{27}$$

was introduced to quatity the maximum force amplification, as an upper bound on the magnitude of the joint forces given an external force or moment. As a bonus, (22) gives an upper bound on applied forces which, in itself, can be used as a dexterity measure. To keep the measure finite, the reciprocal will be taken and it will be scaled, thus a second dexterity measure called *unilateral maximum force amplification* follows:

$$\mathrm{UF_l} \equiv \begin{cases} \sqrt{n+2}\,\sigma_n \dfrac{h_{\min}}{\sqrt{h_{\min}^2 + 1}} & \text{for} \quad h_{\min} \geqslant 0, \\ 0, & \text{when} \quad h_{\min} < 0. \end{cases} \tag{28}$$

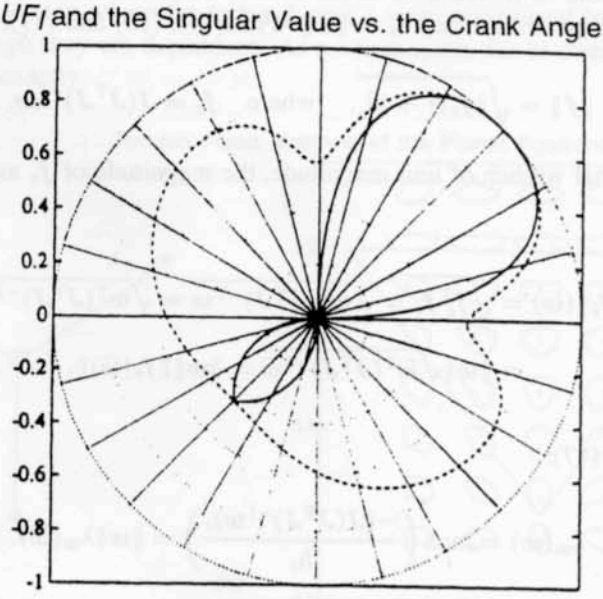

Figure 2. Unilateral dexterity of a tendon actuated crank as a function of the angular variable. The solid line plots $\mathrm{UF_l}$ and the dashed line plots the singular value. In certain regions $\mathrm{UF_l}$ is zero, and the crank can not be moved in both directions with tendons. If pistons were used then the mechanism would always be controllable.

This has the same physical significance as the minimum singular value measure F_1 for ordinary mechanisms. UF_1 is zero at an 'unilateral singularity'. Maximizing this quantity effectively minimizes the tendon forces in a particular configuration. Using F_1 (respectively UF_1) in conjunction with D_1 (respectively UD_1) for any design analysis or control guarantees that the manipulability measure introduced by Yoshikawa [17], in the form of the product or geometrical mean of the singular values, does not vanish.

As an example, Fig. 2 plots the singular value and UF_1 for the tendon–crank system of Fig. 1. Here $n = 1$ so there is only one singular value, thus condition number measures do not apply. Notice there are regions for which UF_1 is zero where the crank cannot be moved in all directions by tendons. If pistons were used then these singularities would not exist as shown by the non-zero singular value.

4. FORCE MAPPING

In this section the tendon dexterity will be interpreted in relation to the force mapping characteristics. For ordinary mechanisms, if the joint forces exist in the unit sphere $\|\boldsymbol{f}\| \leqslant 1$, then the external wrench maps to the ellipsoid $\boldsymbol{w}^{\mathrm{T}}(\boldsymbol{J}^{\mathrm{T}}\boldsymbol{J})^{-1}\boldsymbol{w} \leqslant 1$. It has principal axes in the direction of the eigenvectors of $(\boldsymbol{J}^{\mathrm{T}}\boldsymbol{J})^{-1}$ and magnitudes equal to the corresponding singular value, give or take the unit weighthing matrix we imply in this discussion.

Since unilateral forces impose non-linear constraints, the unit sphere will no longer map to an ellipsoid as it would be in the case of bidirectional actuators. It will map to a truncated shape with radius $r_{\mathrm{u}} = \|\boldsymbol{w}\|$. From (4), (13) and (17),

$$\|\boldsymbol{f}\| = \sqrt{\|\boldsymbol{f}_{\mathrm{e}}\|^2 + \lambda_{\mathrm{m}}^2}, \quad \text{where} \quad \boldsymbol{f}_{\mathrm{e}} = \boldsymbol{J}(\boldsymbol{J}^{\mathrm{T}}\boldsymbol{J})^{-1}\boldsymbol{w}. \tag{29}$$

Call $\widehat{\boldsymbol{w}}$ an external wrench of *unit* magnitude, the magnitude of $\boldsymbol{f}_{\mathrm{e}}$ as a function of $\boldsymbol{f}$ is:

$$\begin{aligned}\|\boldsymbol{f}_{\mathrm{e}}\|(\boldsymbol{w}) &= \sqrt{\boldsymbol{f}_{\mathrm{e}}^{\mathrm{T}}\boldsymbol{f}_{\mathrm{e}}} = \sqrt{\boldsymbol{w}^{\mathrm{T}}(\boldsymbol{J}^{\mathrm{T}}\boldsymbol{J})^{-\mathrm{T}}\boldsymbol{w}} = \sqrt{\boldsymbol{w}^{\mathrm{T}}(\boldsymbol{J}^{\mathrm{T}}\boldsymbol{J})^{-1}\boldsymbol{w}} \\ &= \|\boldsymbol{w}\|\sqrt{\widehat{\boldsymbol{w}}^{\mathrm{T}}(\boldsymbol{J}^{\mathrm{T}}\boldsymbol{J})^{-1}\widehat{\boldsymbol{w}}} = \|\boldsymbol{w}\|\|\boldsymbol{f}_{\mathrm{e}}(\widehat{\boldsymbol{w}})\|. \end{aligned} \tag{30}$$

Similarly, from (17):

$$\lambda_{\mathrm{m}}(\boldsymbol{w}) = \max_i \left(\frac{-(\boldsymbol{J}(\boldsymbol{J}^{\mathrm{T}}\boldsymbol{J})^{-1}\boldsymbol{w})_i}{\boldsymbol{h}_i}\right) = \|\boldsymbol{w}\|\lambda_{\mathrm{m}}(\widehat{\boldsymbol{w}}). \tag{31}$$

From (29), (30) and (31):

$$\|\boldsymbol{f}\| = \|\boldsymbol{w}\|\sqrt{\|\boldsymbol{f}_{\mathrm{e}}(\widehat{\boldsymbol{w}})\|^2 + \lambda(\widehat{\boldsymbol{w}})^2} = \|\boldsymbol{w}\|\sqrt{\widehat{\boldsymbol{w}}^{\mathrm{T}}(\boldsymbol{J}^{\mathrm{T}}\boldsymbol{J})^{-1}\widehat{\boldsymbol{w}} + \lambda(\widehat{\boldsymbol{w}})^2}. \tag{32}$$

Setting the tendon force vector on the unit sphere $\|f\| = 1$, the radius $r_u(J, \widehat{w})$ of the mapped volume is deduced from (32):

$$r_u(J, \widehat{w}) = \frac{1}{\sqrt{\widehat{w}^T (J^T J)^{-1} \widehat{w} + \lambda_m(\widehat{w})^2}}. \tag{33}$$

As an illustration, consider the tendon actuated planar parallel manipulator of Fig. 3(a). It is possible to manipulate objects within the indicated triangle. The force mapping at various points is shown on Fig. 3(b). Directions with a large radius with respect to the origin ('x') are able to transmit large forces in the corresponding direction. Outside the triangle there will be directions for which it is impossible to produce forces. At the centroid of the triangle the manipulator is 'unilaterally isotropic'; however, the force mapping is not circular as one might expect.

Based on the analysis of the previous section,

$$\sigma_1 \geqslant r_{u\,max} \geqslant r_u \geqslant r_{u\,min} \geqslant \frac{\sigma_n h_{min}}{\sqrt{h_{min}^2 + 1}}. \tag{34}$$

Thus from (26), (6):

$$\frac{1}{\sqrt{n+2}} UD_1 \leqslant \frac{r_{u\,min}}{r_{u\,max}}. \tag{35}$$

Notice that the 'unilateral dexterity' is not proportional to the ratio of minimum to maximum radius but does provide a lower bound. This is a result of the simplications of the previous section where the terms f_e and λ were maximized (minimized) separately even though they are dependent. As a comparison, for bi-directional actuators $D_1 = r_{min}/r_{max}$ exactly.

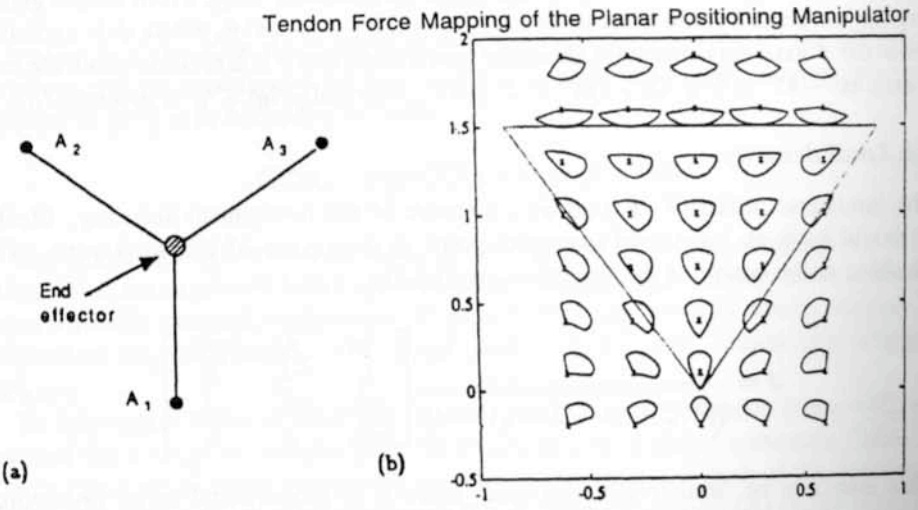

Figure 3. Tendon actuated parallel positioning manipulator (a). The force mapping at various points (b). The origin of each mapping is marked with an 'x'. Outside the indicated triangle the dexterity is zero, but there will be directions for which it is possible to produce forces and others for which it is not.

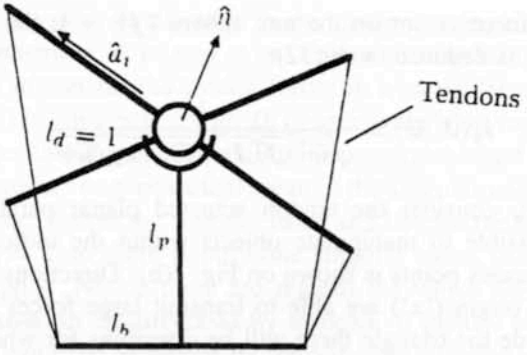

Figure 4. Tendon actuated spherical mechanism with square platform. The design parameters are l_d, l_p, and l_b. Its kinematic properties are determined by two parameters only and l_d is set to 1. $\hat{n}$ is the unit vector pointing out normal to the platform. The $\hat{a}_i$'s are unit vectors pointing from the pivot to the four tendon attach points. The central joint can be implemented as a ball and half socket.

5. APPLICATION: TENDON ACTUATED SPHERICAL MECHANISM

Several interesting n d.o.f. mechanisms can be found that are actuated by $n + 1$ tendons. A seven cable mechanism would be easy to construct, but will have a small workspace, a characteristic shared by all these designs. The dexterity measure of the previous section could be used to optimize any of the unilaterally constraining set of $n + 1$ forces.

For illustration of the proposed measures, a tendon actuated spherical mechanism is now studied that is analogous to the spherical mechanism discussed in [15], with the linear actuators replaced by tendons (Fig. 4). The workspace will not be nearly as large; however, it will be a useful device in cases where tendon actuation is essential.

The workspace is now limited by 'unilateral singularities' only. From simple geometry the workspace given in terms of the Euler angles ψ, ϕ and θ, where ψ is a rotation about the x-axis, ϕ is a rotation about the new y-axis, and θ is a rotation about the new z-axis, is: $-45° \leqslant \theta \leqslant 45°$; $-90° \leqslant \phi \leqslant 90°$; $-\arctan(l_p/l_b) \leqslant \psi \leqslant \arctan(l_p/l_b)$.

5.1. Local dexterity

The 'unilateral dexterity' is used as a measure of the mechanism accuracy. Ideally it should have an 'unilateral isotropic' point as the centre of the workspace. The Jacobian at the centre of the workspace is trivially:

$$J = \frac{1}{\sqrt{1/2 + (1/\sqrt{2} - l_b)^2 + l_p^2}} \begin{bmatrix} l_p & l_p & -l_b \\ l_p & -l_p & l_b \\ -l_p & -l_p & -l_b \\ -l_p & l_p & l_b \end{bmatrix}. \tag{36}$$

This matrix is be 'unilaterally isotropic' when it is proportional to an orthogonal matrix and the columns sum to zero. This happens when $l_p = l_b$.

The 'unilateral dexterity' of the mechanism for various cases was examined ($l_b = l_p = 0.707$, $l_b = l_p = 1$, $l_b = l_p = 5$, Fig. 9, when $l_d = 1$). As expected there is an

'unilaterally isotropic' point for $\psi = \phi = \theta = 0$, and 'unilateral singularity' at the limit of the workspace. In contrast to the bidirectionally actuated counterpart which could be made isotropic in five locations, only one isotropic point was found.

In the next section the geometrical design of this mechanism will be optimized according to its dexterity.

5.2. Optimization of the tendon mechanism

The procedure now outlined to optimize the tendon mechanism is based on the method described in [15]. First, a *unilateral global dexterity* measure $\mathrm{UD_g}$ is defined based on the integral of the local 'unilateral dexterity':

$$\mathrm{UD_g} = \int_{\mathcal{W}} \mathrm{UD_l}\, \mathrm{d}w \approx \frac{1}{N_w} \sum_{w \in \mathcal{W}} \mathrm{UD_l}. \tag{37}$$

Then the integral is approximated by a discrete sum where w is one of N_w equally spaced points in the quaternion unit hypersphere within the workspace $\mathcal{W}$ of the mechanism. The only complicating factor is that the workspace is now a function of the design variables and so the number N_w and the set $\mathcal{W}$ will be changing. Each point must be tested to ensure that it is inside the workspace before the corresponding dexterity is calculated.

One of the goals is to minimize the tension on the tendons, so a secondary objective function based on the integral of $\mathrm{UF_l}$ is introduced: the *unilateral global force amplification*. This can be calculated in the same fashion as measure $\mathrm{UD_g}$ by defining:

$$\mathrm{UF_g} = \int_{\mathcal{W}} \mathrm{UF_l}\, \mathrm{d}w \approx \frac{1}{N_w} \sum_{w \in \mathcal{W}} \mathrm{UF_l}. \tag{38}$$

Finally as a check on the flatness of the local 'unilateral dexterity', the maximum gradient will be investigated leading to the *unilateral maximum dexterity gradient*. Similar to [15], it is defined as follows:

$$\mathrm{GUD_g} = \max_{\mathcal{W}} \mathrm{GUD_l} = \max_{\mathcal{W}} \|\nabla \mathrm{UD_l}\|. \tag{39}$$

The dexterity was maximized using Powell's method with the results given in Table 1. Two maxima were found corresponding to designs that are physically realizable with virtually identical workspaces. Figure 5 plots the dexterity versus the two independent lengths l_b and l_p. The 'ridge' is near the locus of 'unilaterally isotropic' designs.

To help select between these two maxima, the measure of tendon forces $\mathrm{UF_g}$ was plotted for a range of designs (Fig. 6) revealing only a single maximum (Table 2). Unlike the case of its bidirectionally actuated counterpart, the peak of this function is sharp and well defined. This maximum (C) is close to solution (A) of the dexterity, hence (A) is considered the superior of the two designs. From a practical viewpoint it is better to have $l_\mathrm{b}^2 + l_\mathrm{p}^2 > l_\mathrm{d}^2$ so that the mechanism platform does not intersect with

Table 1.
Maximum values of UD_g

	l_b	l_p	UD_g
A	1.024091	1.100127	0.284555
B	0.453248	0.486915	0.284555

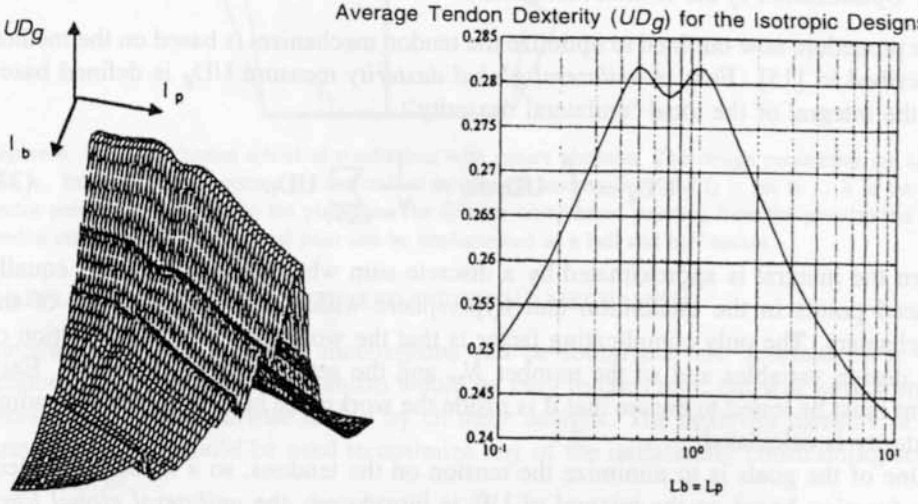

Figure 5. Global tendon dexterity of the parallel mechanism (left). The design lengths l_b and l_p range from 0.1 to 10 on a logarithmic scale. This plot of UD_g reveals two maxima near the curve of isotropic designs (right).

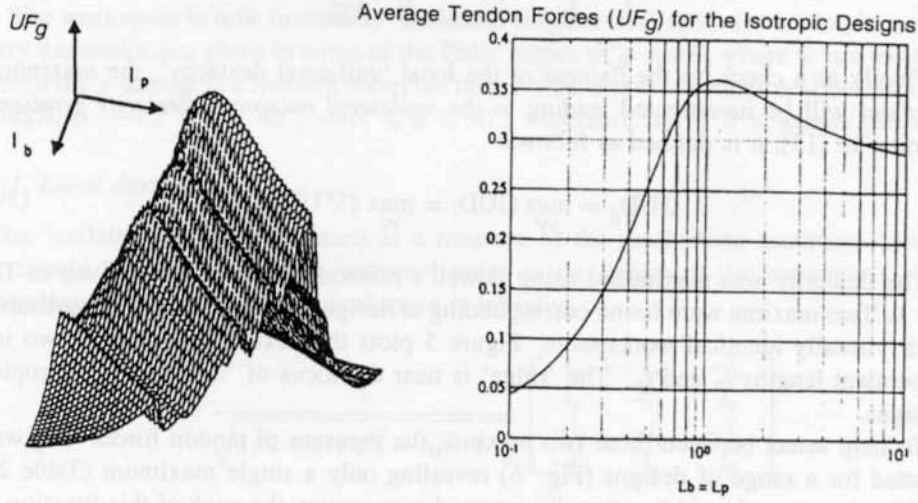

Figure 6. UF_g versus the design variables. When plot against l_b and l_p a single maximum is revealed (left). The 'ridge' lies near the curve of isotropic designs (right).

Table 2.
Maximum value of UF_g

	l_b	l_p	UF_g
C	1.163289	1.297686	0.368784

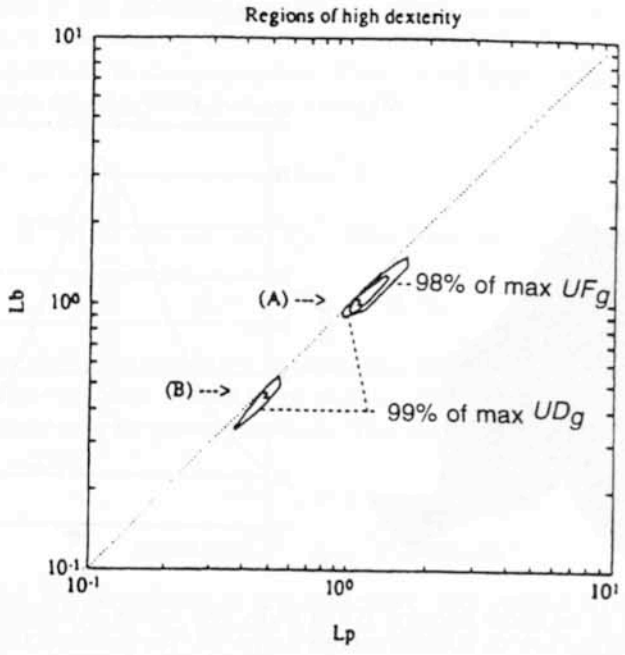

Figure 7. Design choice (A) falls within the 98th percentile of UF_g. Maximum (B) is clearly unacceptable.

the attachment point of the tendons when it is near the boundary of the workspace. In this respect, design (A) is once again superior as it leads to the simplest construction of a compact and dextrous mechanism. As shown in Fig. 7 design (A) falls within the 98th percentile of UF_g and is therefore acceptable in terms of both measures.

The final stage of this analysis is to check the flatness of the 'unilateral dexterity' based on its maximum gradient. Figure 8(a) shows GUD_g over a range of the design variables. The gradient is largest for the isotropic designs, and increases as $l_p = l_b \rightarrow 1/\sqrt{2}$. Notice that the poorest designs with respect to dexterity are those with the flattest and hence smallest gradient. The goal is not to minimize the gradient measure, but to use it to help select between competing alternatives.

Table 3 lists GUD_g for the optimized designs showing that (C) has the smallest response. By examining Fig. 8(b) it is evident that none of these choices has smooth dexterity. According to Fig. 8(b) it would appear that a large value of l_b results in a smooth dexterity function. Two isotropic cases are compared in Fig. 9, one with $l_b = l_p = 1/\sqrt{2}$, and the other with $l_b = l_p = 5$. The isotropic point at the centre of the workspace has the largest gradient, but it does not change significantly between

Table 3.
Value of GUD_g for three design choices

Design	GUD_g
A	29.740265
B	28.983616
C	27.327013

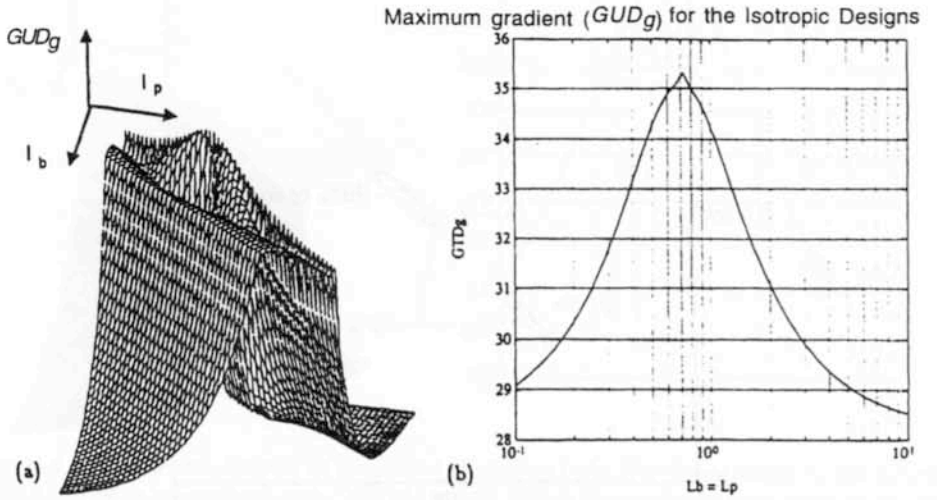

Figure 8. Gradient of the tendon dexterity. Plot of GUD_g over a range of designs (a). The ridge of largest gradient coincides with the extended isotropic designs (b). The gradient is largest in the vicinity of $l_p = l_b = 0.707$.

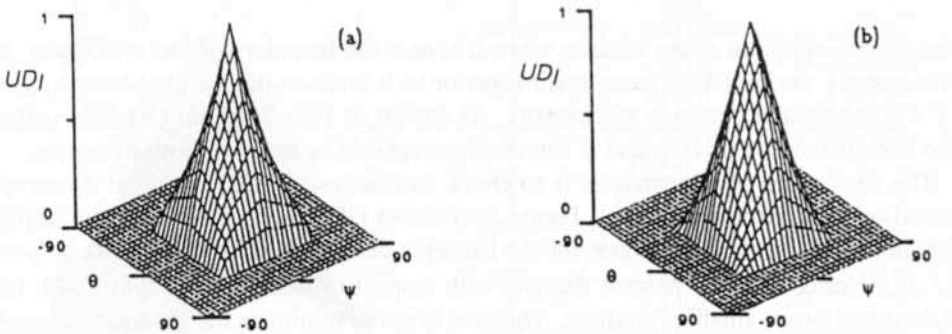

Figure 9. Comparison of the tendon dexterity for two isotropic cases: $l_b = l_p = 0.707$ (a) and $l_b = l_p = 5$ (b), when $\phi = 0$. Both graphs appear very similar.

the two designs. Also, there are no spikes generated as $l_b, l_p \to 1/\sqrt{2}$, a problem that affected the linearly actuated spherical mechanism [15]. Therefore the gradient of the dexterity has little bearing on the optimization of this particular tendon-actuated mechanism.

5.3. Control of internal forces

Internal wrenches refer to the forces and moments experienced at the unactuated joints and supporting structures of the mechanism. From (4) it is apparent that only the forces which map onto the nullspace of the Jacobian can be specified.

For the case of the parallel mechanism it would be useful to have some control over the forces present at the spherical joint. If the spherical joint is constructed from a ball and a socket then stability would result if the force in the normal direction to the mechanism platform is always positive. This normal force, denoted $\boldsymbol{f}_n$, is a linear combination of the tendon forces.

$$\boldsymbol{f}_n = \boldsymbol{g}^T \boldsymbol{f}, \tag{40}$$

where $\boldsymbol{g} = [\hat{a}_1 \cdot \hat{n} \quad \hat{a}_2 \cdot \hat{n} \quad \hat{a}_3 \cdot \hat{n} \quad \hat{a}_4 \cdot \hat{n}]^T$. Thus from (4)

$$\boldsymbol{f}_n = \boldsymbol{g}^T \boldsymbol{J}^+ \boldsymbol{n} + \lambda \boldsymbol{g}^T \widehat{\boldsymbol{h}}. \tag{41}$$

A necessary and sufficient condition to make this force positive is $\boldsymbol{g}^T \widehat{\boldsymbol{h}} > 0$. Since all the components of $\widehat{\boldsymbol{h}}$ are known to be positive, then a sufficient condition is that all the components of $\boldsymbol{g}$ be positive as well. This implies $\hat{a}_1 \cdot \hat{n} > 0$, or expressed in terms of Euler angles,

$$-90^\circ \leqslant \phi \leqslant 90^\circ, \tag{42}$$

$$-\arctan(l_p/l_b) \leqslant \psi \leqslant \arctan(l_p/l_b). \tag{43}$$

These are in fact the boundaries of the workspace with respect to ϕ and ψ of the tendon manipulator; hence, the normal force on the ball joint is always controllable within the workspace of the mechanism.

6. SUMMARY AND CONCLUSION

The statics of unilaterally driven mechanisms have been studied and it was found that dexterity measures such as the condition number of the Jacobian matrix cannot apply to this case. Equivalent measures have been developed and applied to the geometric optimization of a 3 d.o.f. tendon driven spherical mechanism taken as an example.

This theory needs to be extended to more general cases, for example to the case of networks of tendons as proposed by Barbieri and Bergamasco because of its relevance to biomechanics and advanced manipulator design [19].

Acknowledgements

The anonymous reviewers are thanked for their helpful comments. The financial support from NSERC (Natural Sciences and Engineering Research Council of Canada), FCAR (Les Fonds pour la Formation des Chercheurs et l'Aide à la Recherche, Québec) and IRIS (Institute for Robotics and Intelligent Systems Center of Excellence of Canada) is gratefully acknowledged.

REFERENCES

1. J. K. Salisbury and C. Ruoff, "The design and control of a dextrous mechanical hand," in *Proc. ASME Computer Conf.*, San Francisco, 1981.
2. J. Kerr and B. Roth, "Analysis of multifingered hands," *Int. J. Robotics Res.*, vol. 4, no. 4, pp. 3–17, 1986.
3. M. Tsuda, Y. Nakamura and T. Higushi, "High-speed digital controller for magnetic servo levitation of robot mechanisms," in *Experimental Robotics 1*, V. Hayward and O. Khatib, eds, New York: Springer-Verlag, 1990.
4. H. Kimura, Z. Wang and E. Nakano, "Huge object manipulation in space by vehicles," in *Proc. IEEE Int. Workshop on Intelligent Systems and Robots*, Tsuchiura, Japan, pp. 393–397, 1990.
5. S. C. Jacobsen, J. E. Wood, D. F. Knutti and K. B. Biggers, "The UTAH/M.I.T. dextrous hand: work in progress," *Int. J. Robotics Res.*, vol. 3, no. 4, pp. 21–49, 1984.
6. J. Vertut, J. Charles, P. Coiffet and P. Petit, "Advance of the new MA-23 force reflecting manipulation system," in *Proc. CISM-IFToMM Symp.*, Warsaw, 1976.
7. A. Morecki, Z. Busko, H. Gasztold and K. Jaworek, "Synthesis and control of the anthropomorphic two-handed manipulator," in *Proc. 10th Int. Symp. on Industrial Robots*, Milan, pp. 461–474, 1980.
8. K. Takase, H. Inoue, K. Sato and S. Hagihara, "The design of an articulated manipulator with torque control ability," in *Proc. 4th Int. Symp. on Industrial Robots*, Tokyo, 1974.
9. S. Hirose and S. Ma, "Coupled tendondriven multijoint manipulator," in *Proc. IEEE Int. Conf. on Robotics and Automation*, vol. 2, pp. 1268–1275, Sacramento, 1991.
10. Z. Li, P. Hsu and S. Sastry, "Grasping and coordinated manipulation by a multifingered robot hand," *Int. J. Robotics Res.*, vol. 8, no. 4, pp. 33–50, 1989.
11. D. C. Deno, R. M. Murray, K. S. J. Pister and S. S. Sastry, "Fingerlike biomechanical robots," in *Proc. Int. Conf. on Robotics and Automation*, vol. 1, pp. 566–572, Nice, 1992.
12. P. Petreschi, D. Pattichizzo and A. Bicchi, "Articulated structures with tendon actuation for whole-limb manipulation," in *Proc. IEEE Int. Conf. on Robotics and Automation*, vol. 1, pp. 848–873, San Diego, 1994.
13. J. Albus, R. Bostelman and N. Dagalakis, "The NIST robocrane," *J. Robotic Syst.*, vol. 10, no. 5, pp. 704–724, 1993.
14. K. Lakshminarayana, "Mechanics of form closure," in *ASME Design Engineering Technical Conf.*, Paper No. 78-DET-32, Minneapolis, 1978.
15. R. Kurtz and V. Hayward, "Multi-goal optimization of a parallel mechanism with actuator redundancy," *IEEE Trans. Robotics Automat.*, vol. 5, pp. 633–651, 1992.
16. J. K. Salisbury and J. J. Craig, "Articulated hand: force control and kinematic issues," *Int. J. Robotics Res.*, vol. 1, no. 1, pp. 4–17, 1982.
17. T. Yoshikawa, "Analysis and design or articulated robot arms from the viewpoint of dynamic manipulability," in *Robotics Research: The 3rd International Symposium*, O. D. Faugeras and G. Giralt, eds, Cambridge, MA: MIT Press, pp. 273–279, 1986.
18. H. Bruynickx, "Some invariance problems in robotics," *Katholieke Universiteit Leuven, Department of Mechanical Engineering, Tech. Rep. 91R4*, 1991.
19. B. Barbieri and M. Bergamasco, "Nets of tendons and actuators: an anthropomorphic model for the actuation system of dextrous robot hands," in *Proc. Fifth Int. Conf. on Advanced Robotics*, vol. 1, New York: IEEE Press, pp. 357–361, 1991.

ABOUT THE AUTHORS

Ronald Kurtz completed his Master's degree in Electrical Engineering at the Center for Intelligence Machines (CIM) at McGill University in 1989. There he specialized in the design optimization of parallel mechanisms with redundancy. Since then, he has been employed at Vadeko Agra Technologies, Toronto, where he develops control systems for large-scale industrial robot manipulators.

Vincent Hayward received the Diplôme d'Ingénieur from Ecole Nationale Supérieure de Mécanique de Nantes, France, and the Diplôme de Docteur-Ingénieur from Université de Paris XI at Orsay in Computer Science, in 1978 and 1981, respectively. He held research positions at Purdue University, Indiana, USA, and at Centre National de la Recherche Scientifique (CNRS), France, and is now Associate Professor with the Department of Electrical Engineering at McGill University, Canada. His contributions include RCCL and Kali, robot control and programming systems now widely used in many application areas. His current research interests and publications are in the following areas: robot trajectory calculation and collision avoidance, and high performance manipulators.